9336 *Inorg. Chem.* **2009**, *48*, 9336–9344
DOI: 10.1021/ic9013043

Inorganic Chemistry
Article

The Crystal Structure of α-K_3AlF_6: Elpasolites and Double Perovskites with Broken Corner-Sharing Connectivity of the Octahedral Framework

Artem M. Abakumov,*,†,§ Graham King,‡ Veronika K. Laurinavichute,§ Marina G. Rozova,§ Patrick M. Woodward,‡ and Evgeny V. Antipov§

†*EMAT, University of Antwerp, Groenenborgerlaan 171, B-2020 Antwerp, Belgium,* ‡*Department of Chemistry, The Ohio State University, 100 West 18th Avenue, Columbus, Ohio 43210-1185, and* §*Department of Chemistry, Moscow State University, Moscow 119992, Russia*

Received July 6, 2009

The crystal structure of α-K_3AlF_6 was solved and refined from a combination of powder X-ray and neutron diffraction data (a = 18.8385(3)Å, c = 33.9644(6)Å, S.G. $I4_1/a$, Z = 80, R_P(X-ray) = 0.037, R_P(neutron) = 0.053). The crystal structure is of the $A_2BB'X_6$ elpasolite type with the $a = b \approx a_e\sqrt{5}$, $c = 4a_e$ superstructure (a_e, parameter of the elpasolite subcell) and rock-salt-type ordering of the K and Al cations over the B and B′ positions, respectively. The remarkable feature of α-K_3AlF_6 is a rotation of 2/5 of the AlF_6 octahedra by $\sim\pi/4$ around one of the crystal axes of the elpasolite subcell, coinciding with the 4-fold symmetry axes of the AlF_6 octahedra. The rotation of the AlF_6 octahedra replaces the corner-sharing between the K and Al polyhedra by edge-sharing, resulting in an increase of coordination numbers of the K cations at the B positions up to 7 and 8. Due to significant deformations of the K polyhedra, the corner-sharing connectivity of the octahedral elpasolite framework is broken and the rotations of the AlF_6 octahedra do not have a cooperative character. Elpasolites and double perovskites with similar structural organization are discussed. The difference in ionic radii of the B and B′ cations as well as the tolerance factor are proposed to be the parameters governing the formation of elpasolites and double perovskites with broken corner-sharing connectivity of the octahedral framework.

1. Introduction

The crystal structures of elpasolites (complex fluorides $A_2BB'F_6$, named after the K_2NaAlF_6 elpasolite) and double perovskites (complex oxides $A_2BB'O_6$, named after the $CaTiO_3$ perovskite) are based on the perovskite structure, where the B and B′ cations are ordered in a chess-board (rock salt) manner, resulting in a $Fm\bar{3}m$ cubic structure with $a_e = 2a_p$ (where a_p is the length of the ABX_3 perovskite subcell edge) (Figure 1). This B-site ordering is driven by size and charge difference between the B and B′ cations.[1] The BX_6 and $B'X_6$ (X = O, F) octahedra are linked by common corners into a network, where the A cations occupy 12-coordinated cavities. A mismatch between the A−X and B(B′)−X interatomic distances results in structural distortions in elpasolites and double perovskites. If the A cation is too small for the 12-coordinated cavity formed by corner-sharing BX_6 and $B'X_6$ octahedra, the octahedral framework undergoes a tilting distortion with bending B−X−B′ bonds and a reduced volume of the coordination polyhedron of the A cation and its coordination number. Possible patterns of corner-linked tilting distortions are restricted by the fact that the octahedral units behave as rigid bodies and the corner sharing of the octahedra is maintained at reasonably small tilt angles ($< 20^o$). That is, the octahedral tilting occurs in a cooperative manner. The corner-linked tilting distortions for the B-site ordered $A_2BB'X_6$ compounds are enumerated using a group theory analysis, including derivations of superstructure unit cells, space symmetry, and phase transition paths between different tilting modes.[2−5]

However, some of the elpasolite-type compounds, such as α-K_3AlF_6 and $K_3MoO_3F_3$, demonstrate superstructures which cannot be attributed to any of the cooperative tilt systems. Electron diffraction investigation revealed that both compounds at room temperature have a tetragonal (or monoclinically distorted pseudotetragonal) supercell with

*To whom correspondence should be addressed. Tel.: +32(3) 2653259. Fax: +32(3) 2653257. E-mail: artem.abakumov@ua.ac.be.

(1) Anderson, M. T.; Greenwood, K. B.; Taylor, G. A.; Poeppelmeier, K. R. *Prog. Solid State Chem.* **1993**, *22*, 197–233.
(2) Howard, C. J.; Kennedy, B. J.; Woodward, P. M. *Acta Crystallogr.* **2003**, *B59*, 463–471.
(3) Flerov, I. N.; Gorev, M. V.; Aleksandrov, K. S.; Tressaud, A.; Grannec, J.; Couzi, M. *Mater. Sci. Eng.* **1998**, *R24*, 81–151.
(4) Aleksandrov, K. S.; Misyul, S. V. *Sov. Phys. Crystallogr.* **1981**, *26*, 612–618.
(5) Stokes, H. T.; Kisi, E. H.; Hatch, D. M.; Howard, C. J. *Acta Crystallogr.* **2002**, *B58*, 934–938.
(6) Abakumov, A. M.; Rossell, M. D.; Alekseeva, A. M.; Vassiliev, S. Yu.; Mudrezova, S. N.; Van Tendeloo, G.; Antipov, E. V. *J. Solid State Chem.* **2006**, *179*, 421–428.

 Published on Web 09/03/2009

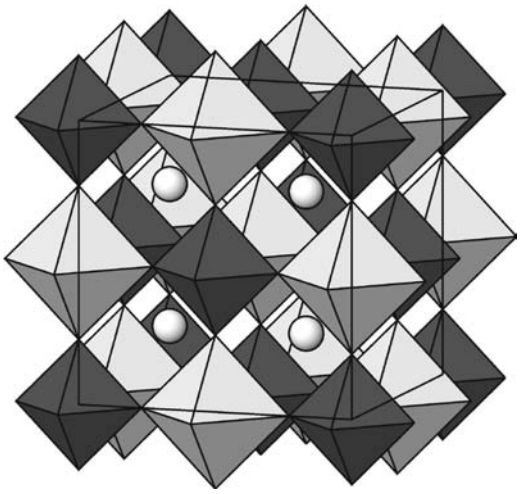

Figure 1. The crystal structure of the cubic $A_2BB'X_6$ elpasolites and double perovskites. Larger B cations are situated at the centers of the gray BX_6 octahedra; the smaller $B'X_6$ octahedra are darker shaded. The A cations are shown as spheres.

$a = b \approx a_e\sqrt{5}$ and $c = 4a_e$, but the origin of this superstructure is still unclear.[6,7] Taking into account the large difference in the size of the B = K and B′ = Al and Mo cations, it was suggested that only the $B'X_6$ octahedra behave as rigid units, whereas the coordination polyhedron around the B cation can be subjected to significant deformations, thus breaking the corner connectivity of the octahedral framework.[6−8] A clue to a possible mechanism of this distortion was given by the structural analysis of the elpasolite-type Rb_2KCrF_6 and Rb_2KGaF_6 complex fluorides.[9] It suggests that a fraction of the $B'F_6$ (B′ = Cr, Ga) octahedra rotate as rigid bodies by $\pi/4$ (the limiting tilt angle for an octahedron) around the four-fold octahedral symmetry axis, changing the coordination environment of part of the B = K cations from octahedral to pentagonal bipyramidal.[9] In this contribution, we demonstrate that a very similar structural mechanism is realized in the α-K_3AlF_6 structure. Extensive microtwinning, arising from phase transitions that occur upon cooling from the high-temperature polymorph, has hampered efforts to use single crystals for structure solution. In this manuscript, we report the use of rigid body constraints to solve the structure of α-K_3AlF_6 from X-ray and neutron powder diffraction data. We also discuss rotation modes of the octahedral units and the structural parameters governing the formation of elpasolites and double perovskites with broken corner-sharing connectivity of the octahedral framework.

2. Experimental Section

The K_3AlF_6 sample was prepared from anhydrous AlF_3 ("Reakhim", "pure" purity grade) and KF. The raw AlF_3 was annealed at 300 °C for 12 h to remove possible traces of absorbed water. Anhydrous KF was prepared by a dehydration of $KF \cdot 2H_2O$ ("Reakhim", "pure for analysis" purity grade) at 500 °C. The purity of the initial materials was confirmed using X-ray powder diffraction. A sample with an overall mass of 12 g and a $KF/AlF_3 = 3.1{:}1$ ratio was prepared, placed in a glassy carbon crucible, melted at 1000 °C for 1.5 h, and cooled down to room temperature with a 100 °C/h cooling rate. The crystallized melt was crushed, and the excess of KF was removed by washing with distilled water.

The X-ray powder diffraction (XRPD) data for structure analysis were collected with a STADI-P diffractometer (Cu $K_{\alpha 1}$ radiation, curved Ge monochromator, transmission mode, linear PSD). Time-of-flight neutron powder diffraction (NPD) data were collected at the HRPD beamline at the ISIS facility of the Rutherford Appleton Laboratory in the United Kingdom. Because of significant peak overlap arising from the very large unit cell volume, only the high-resolution 168° databank was used in the refinement. The JANA2006 program package was used for the structure determination and joint Rietveld refinement from XRPD and NPD data.[10]

3. Results

According to the results of a previous electron diffraction (ED) investigation,[6] the unit cell vectors of α-K_3AlF_6 are related to the unit cell vectors of the cubic elpasolite structure with $a_e \approx 8.5$ Å by a transformation matrix:

$$\begin{pmatrix} 1 & 2 & 0 \\ -2 & 1 & 0 \\ 0 & 0 & 4 \end{pmatrix}$$

This results in a tetragonal unit cell with $a = b \approx a_e\sqrt{5}$ and $c = 4a_e$. The reflection conditions hkl, $h + k + l = 2n$; $hk0$, $h,k = 2n$, observed with ED, leave the space group $I4_1/a$ as the only possibility. The reflection positions and intensity distribution on the ED patterns match well with the $4/m$ point group, but a slight monoclinic distortion with very close a and b parameters and the γ angle slightly deviating from 90° could not be excluded (we will keep the monoclinic first setting (γ setting) for easy transition between the tetragonal and monoclinic unit cells). A small monoclinic distortion was also found for $K_3MoO_3F_3$; this room-temperature polymorph demonstrates the same superstructure as α-K_3AlF_6.[7] Thus, $I112/b$ and $I11b$ (nonstandard settings of the space groups $C2/c$ (no. 15) and Cc (no. 9), respectively) monoclinic subgroups of $I4_1/a$, matching the experimentally observed reflection conditions, should also be taken into account for constructing initial structure models. It should be noted that the $I4_1/a$ space group does not have subgroups within the orthorhombic crystal system.

The starting models used for the Rietveld refinement were constructed by considering different possibile arrangements of the symmetry elements in the supercell with respect to the atomic positions in the basic cubic $Fm\bar{3}m$ elpasolite $A_2BB'X_6$ structure. The elpasolite structure has three positions of inversion centers: at 0,0,0, which is the 4*a* position of the B cation; at 1/2,1/2,1/2, which is the 4*b* position of the B′ cation; and at 0,1/4,1/4, the 24*d* position, which is not associated with atomic entities. These positions can be chosen as an origin for the tetragonal $I4_1/a$ supercell. Fixing the origin to the 0,1/4,1/4 position of the cubic subcell results in the structure shown in Figure 2a along with the positions of inversion centers and four-fold axes of the $I4_1/a$ space group. The second setting of the $I4_1/a$ space group was chosen because the structure can be

(7) Brink, F. J.; Withers, R. L.; Friese, K.; Madariaga, G.; Noren, L. *J. Solid State Chem.* **2002**, *163*, 267–274.
(8) Withers, R. L.; Welberry, T. R.; Brink, F. J.; Noren, L. *J. Solid State Chem.* **2003**, *170*, 211–220.
(9) Zuniga, F. J.; Tressaud, A.; Darriet, J. *J. Solid State Chem.* **2006**, *179*, 3607–3614.
(10) Petricek, V.; Dusek, M. *JANA2000*; Institute of Physics: Praha, Czech Republic, 2000.

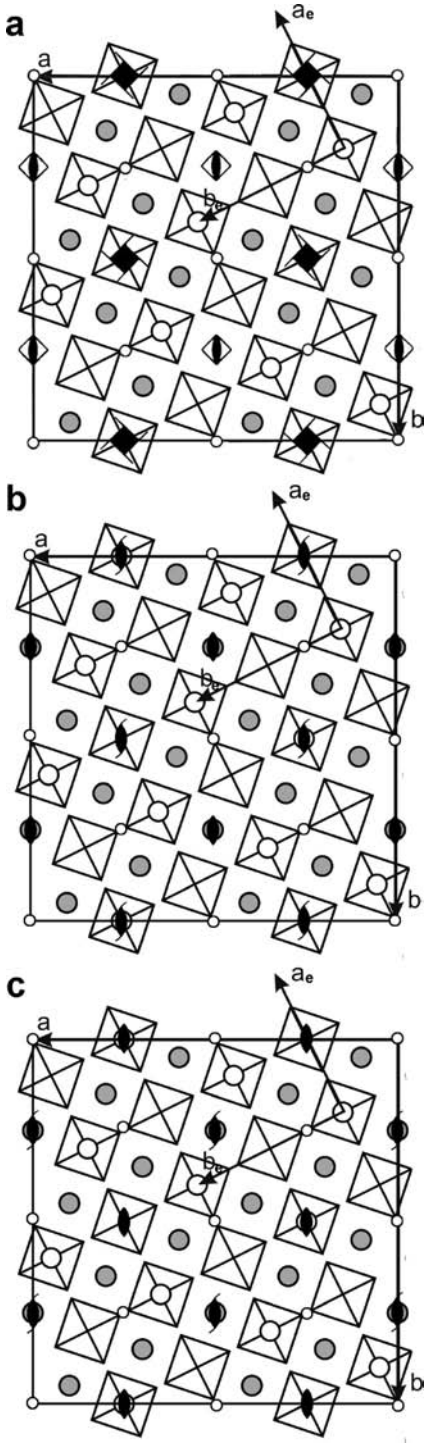

Figure 2. The projection of the parent elpasolite structure within the $a = b \approx a_e\sqrt{5}$, $c = 4a_e$ supercell with overlaid positions of symmetry axes and inversion centers of the $I4_1/a$ (a), $I112/b$ (b), and $I112/a$ (c) space groups. The $B'X_6$ octahedra are shown; the A and B cations are shown as empty and gray circles, respectively. The notations for symmetry elements correspond to those in the International Tables for Crystallography.

transformed to the $I2/b$ subgroup without shifting the origin. It is also obvious from Figure 2 that fixing the origin to either 0,0,0 or to 1/2,1/2,1/2 subcell positions would result in the four-fold axes of the $I4_1/a$ space group passing through the 1/4,0,0 and 0,1/4,0 24*e* positions of the cubic subcell with the point symmetries 4*mm* and *m*4*m*, respectively, which does not match the four-fold axes parallel to the *c* axis. Thus, the location of the origin at the 0,1/4,1/4 or symmetrically equivalent subcell position is the unique choice, and the other possibilities can be discarded. In the resulting structure, the 4_1 screw axes pass through the columns of the alternating corner-sharing BX_6 and $B'X_6$ octahedra, whereas the $\bar{4}$ inversion axes pass through the columns of the A cations. Reducing the symmetry from $I4_1/a$ to $I112/b$ is then straightforward and requires a replacement of the 4_1 screw axes with the 2_1 screw axes and the $\bar{4}$ inversion axes with 2-fold rotation axes (Figure 2b). By an origin shift over the [1/4,1/4,1/4] vector of the supercell, a second possible structure can be obtained with the $I112/a$ space group, where the 2_1 screw axes are located at the A-cation columns and 2-fold rotation axes − at the octahedral columns (Figure 2c). Although both monoclinic structures have the same unit cell and space group, they are different because the site symmetry of the B and B′ cations at the 1/4,0,*z* position of the supercell is 1 in the $I2/b$ structure and 2 in the $I2/a$ structure. It should be noted that fixing the origin to either the 0,0,0 or 1/2,1/2,1/2 subcell position is also not allowed in both $I2/b$ and $I2/a$ structures. In the acentric space group Ib, the origin position is not fixed in the *ab* plane and can be chosen arbitrarily.

The symmetry analysis resulted in four models ($I4_1/a$, $I2/b$, $I2/a$, and Ib), which should be verified with Rietveld refinement. However, even the most symmetric $I4_1/a$ model contains 53 symmetrically independent atoms with 147 refined atomic coordinates. Taking into account additional difficulties arising from extensive peak overlap due to the very large unit cell volume (> 12 000 Å^3), some approximations must be made to reduce the number of refined parameters, at least at the first stage of the refinement. As suggested earlier,[6−8] in the $K_3MoO_3F_3$ and α-K_3AlF_6 structures, the $B'X_6$ (B′ = Mo, Al; X = O, F) octahedra behave like rigid units, whereas rigid unit behavior does not necessarily occur for the KX_6 octahedra with significantly larger K−X separation. The rigid body approximation then looks plausible to describe displacements and rotations of the AlF_6 octahedral units in α-K_3AlF_6.

In the $I4_1/a$ model, there are five symmetrically independent Al atoms located at general 16*f* positions. Thus, 105 variable atomic coordinates are required to describe the positions and orientation of the AlF_6 octahedra. Each octahedron can be described by a position of its center (the Al atom) and three rotation angles defining the orientation of the local coordinate system of the octahedron with respect to the crystal axes (see Petricek and Dusek[11] for more details). This reduces the amount of refined parameters to 30 for the AlF_6 octahedra. Additionally, 42 refined atomic coordinates are necessary to describe the positions of the K atoms.

The positions and rotation angles of the AlF_6 units reproducing the octahedral arrangement in the cubic elpasolite structure were chosen for the starting $I4_1/a$ model. The Al−F distance was set to be equal to 1.80 Å. The refinement was performed first from XRPD data only. The positions of the K atoms at the A sites, the positions of the K atoms at the B sites, the positions of the centers of the AlF_6 octahedra, and their rotation angles were subsequently included into the refinement. After the achievement of convergence, the

(11) Petricek, V.; Dusek, M. *JANA98: The Crystallographic Computing System, Manual*; Institute of Physics: Praha, Czech Republic, 1998.

high-resolution NPD data bank was added, and the refinement was performed from joint XRPD and NPD data sets. At the final stage, the Al−F distances were included in the refinement. The residual reliability factors revealed an acceptable agreement between the experimental and calculated diffraction profiles ($R_F = 0.060$ and $R_P = 0.038$ for the XRPD data and $R_F = 0.055$ and $R_P = 0.058$ for the NPD data). In order to ensure that the obtained structure is unique, the structure solution using a Monte Carlo based global optimization was undertaken using the FOX program.[12] The rotation angles of the AlF_6 octahedra were selected as variable parameters. The optimization revealed the same structure as the one obtained from the Rietveld refinement.

Decreasing the symmetry down to the $I2/b$ subgroup decreases the reliability factors ($R_F = 0.053$ and $R_P = 0.036$ for the XRPD data and $R_F = 0.039$ and $R_P = 0.052$ for the NPD data). However, the resulting atomic arrangement reproduces the $I4_1/a$ model. Moreover, the a and b lattice parameters stay equal in the range of standard deviation, and the monoclinic angle γ was found to be equal to 90° (a = 18.8396(5)Å, b = 18.8388(5)Å, c = 33.9657(6)Å, and γ = 90.000(2)°). The standard deviations of the atomic coordinates of the K atoms, symmetrically equivalent in the $I4_1/a$ model, become twice as large on going to the $I2/b$ subgroup, indicating the absence of a noticeable deviation from the $I4_1/a$ symmetry. For the refinement of the $I2/a$ model, the AlF_6 octahedra were split into two groups: with centers positioned at the general 8*f* position and with centers at the 4*e* position. The site symmetry of the 4*e* position is 2, and this two-fold axis can pass either through two trans vertices or through the midpoints of the opposite edges of the AlF_6 octahedra. Monte Carlo based global optimization was also performed, and different combinations of octahedral tilts were tried that finally resulted in the reliability factors $R_F = 0.068$ and $R_P = 0.045$ for the XRPD data and $R_F = 0.056$ and $R_P = 0.072$ for the NPD data, significantly higher than those for the $I2/b$ and $I4_1/a$ models. Thus, the $I2/a$ model was discarded. The refinement in the acentric Ib space group does not converge. Even if some structure distortion is present, eliminating the inversion center, in this particular case, the detection of this distortion is beyond the capabilities of powder diffraction.

The $I4_1/a$ structure was chosen for final refinement. For the final refinement, the rigid body coordinates were transformed into conventional atomic coordinates, which were refined without any other constrains. An overall atomic displacement parameter was refined ($U = 0.0085(2)$Å^2). The crystallographic data of α-K_3AlF_6 are summarized in Table 1. The relevant interatomic distances are listed in Table 2. Experimental, calculated, and difference XRPD and NPD profiles are shown in Figure 3a and b, respectively. The positional parameters for the α-K_3AlF_6 structure are listed in Table 1 of the Supporting Information.

An overview of the α-K_3AlF_6 crystal structure is shown in Figure 4. The cation positions in this structure roughly correspond to the cation positions in the cubic elpasolite structure: the A positions are occupied by the K cations (K(1)−K(13), denoted further as K_A), and the B and B′ positions are occupied in a chess-board ordered manner by the K cations (K(14)−K(18), denoted further as K_B) and Al cations, respectively. The Al cations are situated in an octahedral fluorine environment with an average Al−F interatomic distance of 1.81 Å. The BVS values for the Al cations, calculated with the parameters given by Brown and Altermatt,[13] vary in the range of 2.74−3.11 with an average value of 2.92, which is in good agreement with the nominal valence. The remarkable difference between the cubic elpasolite structure and α-K_3AlF_6 is a rotation of 2/5 of the AlF_6 octahedra by an angle of $\pi/4$ around one of the crystal axes of the elpasolite subcell (coinciding with the 4-fold symmetry axes of the AlF_6 octahedra). This results in a drastic change of the coordination polyhedra of the K_B cations. The rotation of the AlF_6 octahedra replaces the corner-sharing between the K_B and Al polyhedra by edge-sharing that increases the coordination number of the K_B cations. If one out of six AlF_6 octahedra surrounding the K_B atom rotates over $\pi/4$, the fluorine octahedron around the K_B atom is transformed into a distorted pentagonal bipyramid with CN = 7 (Figure 5a). This coordination is realized for two K_B atoms, K(17) and K(18). The average K−F interatomic distance for these positions is 2.65 Å. For these atoms, the BVS values, calculated with the parameters given by Adams,[14] are larger than the nominal valence (1.26 for K(17) and 1.09 for K(18)), indicating that they remain slightly overbonded. For the K_B atoms K(14)−K(16), two AlF_6 octahedra in cis positions are rotated over $\pi/4$ around mutually perpendicular axes, which results in an 8-fold polyhedron (a capped pentagonal bipyramid). The average K−F interatomic distance of 2.77 Å for these positions is larger than that for the 7-fold coordinated K_B positions. However, for the K(14)−K(16) atoms, one K−F interatomic distance (3.08−3.20 Å) is noticeably larger than the average distance, so that the coordination number of these cations is better described as 7 + 1. For the K14−K16 atoms, the BVS values are in the range of 0.97−1.01, in perfect agreement with the nominal value.

In order to represent the ordering pattern of the rotated AlF_6 octahedra, it is more convenient to consider the structure as consisting of octahedral layers, alternating along the c axis and positioned at $z \approx (2n + 1)/16$ ($n = 0-7$). In every layer, there are 10 AlF_6 octahedra, six of which nearly retain their orientation with respect to the elpasolite crystal axes (marked as 0 in Figure 6), two are rotated by $\sim\pi/4$ around the c_e axis (marked as c in Figure 6), and two are rotated by $\sim\pi/4$ around either the a_e or b_e axis (marked as a or b in Figure 6, respectively). The layers are symmetry related by operations of the $I4_1/a$ space group.

Table 1. Selected Parameters from the Rietveld Refinement of α-K_3AlF_6

formula	K_3AlF_6
space group	$I4_1/a$
a, Å	18.8385(3)
c, Å	33.9644(6)
Z	80
cell volume, Å^3	12053.6(3)
calcd density, g/cm^3	2.845
overall U, Å^2	0.0085(2)
XRPD data set:	
radiation	$CuK_{\alpha 1}$, λ = 1.5406 Å
2θ range; step, deg	$10 \le 2\theta \le 100$; 0.01
R_F, R_P, R_{wP}	0.058, 0.037, 0.049
NPD data set:	
d range, Å	0.725−2.61
R_F, R_P, R_{wP}	0.046, 0.053, 0.057
params refined	148
GOF	1.63

(12) Favre-Nicolin, V.; Černy, R. *J. Appl. Crystallogr.* **2002**, *35*, 734–743.
(13) Brown, I. D.; Altermatt, D. *Acta Crystallogr.* **1985**, *B41*, 244–247.
(14) Adams, S. *Acta Crystallogr.* **2001**, *B57*, 278–287.

Table 2. Selected Interatomic Distances for α-K_3AlF_6 (Å)

		K_A cations			
K(1)−F(14)	2.61(1)×2	K(2)−F(11)	2.50(1)×1	K(3)−F(11)	2.50(1)×1
K(1) − F(15)	3.10(1)×2	K(2)−F(12)	2.72(1)×1	K(3)−F(15)	2.97(1)×1
K(1)−F(22)	2.65(2)×2	K(2)−F(13)	2.64(1)×1	K(3)−F(32)	2.90(1)×1
K(1)−F(23)	3.04(1)×2	K(2)−F(31)	2.58(2)×1	K(3)−F(33)	2.64(2)×1
K(1)−F(24)	2.85(1)×2	K(2)−F(33)	2.84(1)×1	K(3)−F(34)	3.00(1)×1
		K(2)−F(35)	2.74(1)×1	K(3)−F(41)	2.83(1)×1
		K(2)−F(45)	2.58(1)×1	K(3)−F(51)	2.85(1)×1
		K(2)−F(46)	2.87(1)×1	K(3)−F(52)	2.73(1)×1
				K(3)−F(53)	2.74(1)×1
K(4)−F(12)	2.87(1)×1	K(5)−F(15)	2.72(1)×1	K(6)−F(13)	2.57(1)×2
K(4)−F(16)	2.81(1)×1	K(5)−F(16)	2.60(1)×1	K(6)−F(33)	3.03(1)×2
K(4)−F(31)	2.98(1)×1	K(5)−F(21)	2.85(1)×1	K(6)−F(34)	2.70(1)×2
K(4)−F(32)	2.80(1)×1	K(5)−F(22)	3.09(1)×1	K(6)−F(35)	2.92(1)×2
K(4)−F(34)	2.86(1)×1	K(5)−F(23)	2.69(1)×1		
K(4)−F(35)	2.68(1)×1	K(5)−F(42)	2.78(1)×1		
K(4)−F(36)	2.78(1)×1	K(5)−F(51)	2.91(1)×1		
K(4)−F(36)	2.73(1)×1	K(5)−F(52)	2.73(1)×1		
K(4)−F(41)	2.55(1)×1	K(5)−F(56)	2.93(1)×1		
K(7)−F(14)	2.49(1)×1	K(8)−F(34)	2.946(9)×4	K(9)−F(21)	3.00(1)×1
K(7)−F(23)	3.00(1)×1	K(8)−F(35)	3.00(1)×4	K(9)−F(21)	2.75(1)×1
K(7)−F(24)	2.92(1)×1	K(8)−F(36)	2.879(9)×4	K(9)−F(22)	3.04(1)×1
K(7)−F(31)	2.78(1)×1			K(9)−F(25)	3.05(1)×1
K(7)−F(32)	2.74(1)×1			K(9)−F(26)	2.82(1)×1
K(7)−F(36)	2.99(1)×1			K(9)−F(26)	2.95(1)×1
K(7)−F(43)	2.75(1)×1			K(9)−F(42)	2.69(1)×1
K(7)−F(45)	2.78(1)×1			K(9)−F(53)	2.91(1)×1
				K(9)−F(55)	2.76(1)×1
K(10)−F(24)	2.91(1)×1	K(11)−F(22)	2.83(1)×2	K(12)−F(21)	2.74(1)×1
K(10)−F(25)	2.86(1)×1	K(11)−F(24)	2.88(1)×2	K(12)−F(23)	2.89(1)×1
K(10)−F(26)	2.85(1)×1	K(11)−F(26)	3.09(1)×2	K(12)−F(25)	2.87(1)×1
K(10)−F(31)	2.99(1)×1	K(11)−F(54)	2.79(1)×2	K(12)−F(43)	3.00(1)×1
K(10)−F(32)	3.07(1)×1			K(12)−F(44)	2.44(1)×1
K(10)−F(33)	2.92(1)×1			K(12)−F(52)	3.08(1)×1
K(10)−F(34)	2.66(1)×1			K(12)−F(55)	2.77(1)×1
K(10)−F(36)	2.72(1)×1			K(12)−F(56)	2.73(1)×1
K(10)−F(52)	3.04(1)×1				
K(10)−F(54)	3.03(1)×1				
K(13)−F(55)	3.01(1)×4				
K(13)−F(56)	2.874(9)×4				
		K_B cations			
K(14)−F(14)	3.08(1)×1	K(15)−F(13)	2.89(1)×1	K(16)−F(11)	2.80(1)×1
K(14)−F(16)	2.80(1)×1	K(15)−F(14)	2.80(1)×1	K(16)−F(12)	2.42(1)×1
K(14)−F(22)	2.54(1)×1	K(15)−F(15)	2.74(1)×1	K(16)−F(13)	3.20(1)×1
K(14)−F(24)	2.81(1)×1	K(15)−F(23)	2.37(1)×1	K(16)−F(34)	2.59(1)×1
K(14)−F(32)	2.54(1)×1	K(15)−F(33)	2.64(1)×1	K(16)−F(35)	2.77(1)×1
K(14)−F(41)	2.82(1)×1	K(15)−F(43)	3.10(1)×1	K(16)−F(36)	2.71(1)×1
K(14)−F(42)	2.78(1)×1	K(15)−F(45)	2.78(1)×1	K(16)−F(41)	2.89(1)×1
K(14)−F(53)	2.74(1)×1	K(15)−F(52)	2.86(1)×1	K(16)−F(45)	2.75(1)×1
K(17)−F(11)	2.94(1)×1	K(18)−F(21)	2.56(1)×1		
K(17)−F(16)	2.82(1)×1	K(18)−F(26)	2.48(1)×1		
K(17)−F(25)	2.76(1)×1	K(18)−F(42)	2.88(1)×1		
K(17)−F(31)	2.75(1)×1	K(18)−F(44)	2.84(1)×1		
K(17)−F(43)	2.54(1)×1	K(18)−F(54)	2.45(1)×1		
K(17)−F(46)	2.50(1)×1	K(18)−F(55)	2.85(1)×1		
K(17)−F(51)	2.18(1)×1	K(18)−F(56)	2.57(1)×1		
		Al cations			
Al(1)−F(11)	1.81(2)×1	Al(2)−F(21)	1.81(2)×1	Al(3)−F(31)	1.80(2)×1
Al(1)−F(12)	1.82(2)×1	Al(2)−F(22)	1.76(2)×1	Al(3)−F(32)	1.79(2)×1
Al(1)−F(13)	1.82(2)×1	Al(2)−F(23)	1.79(2)×1	Al(3)−F(33)	1.76(2)×1
Al(1)−F(14)	1.86(2)×1	Al(2)−F(24)	1.88(2)×1	Al(3)−F(34)	1.82(2)×1
Al(1)−F(15)	1.76(2)×1	Al(2)−F(25)	1.81(2)×1	Al(3)−F(35)	1.87(2)×1
Al(1)−F(16)	1.80(2)×1	Al(2)−F(26)	1.84(2)×1	Al(3)−F(36)	1.86(2)×1
Al(4)−F(41)	1.83(2)×1	Al(5)−F(51)	1.75(2)×1		
Al(4)−F(42)	1.79(2)×1	Al(5)−F(52)	1.85(2)×1		
Al(4)−F(43)	1.86(2)×1	Al(5)−F(53)	1.88(2)×1		
Al(4)−F(44)	1.84(2)×1	Al(5)−F(54)	1.79(2)×1		
Al(4)−F(45)	1.87(2)×1	Al(5)−F(55)	1.76(2)×1		
Al(4)−F(46)	1.83(2)×1	Al(5)−F(56)	1.74(2)×1		

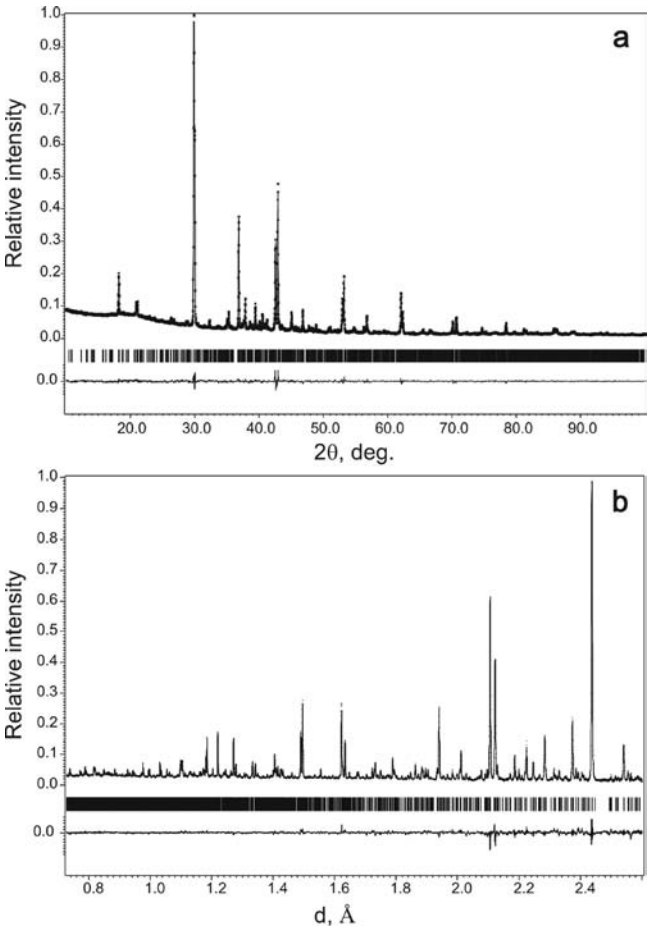

Figure 3. Experimental, calculated, and difference XRPD (a) and NPD (b) profiles.

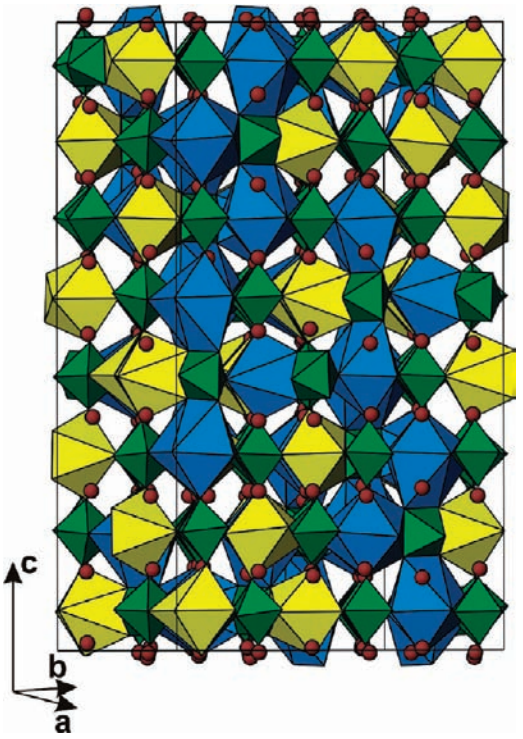

Figure 4. The crystal structure of α-K_3AlF_6. The AlF_6 octahedra are green; the K_BF_7 and K_AF_8 polyhedra are yellow and blue, respectively. The K_A cations are shown as brown spheres.

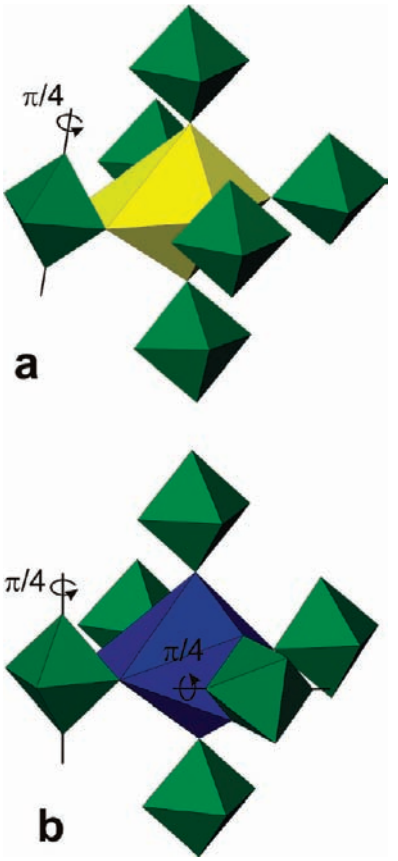

Figure 5. A formation of the K_BF_7 (a) and K_AF_8 (b) polyhedra as a result of rotation of the AlF_6 octahedra (green) over ~$\pi/4$.

Due to rotations of the AlF_6 octahedra, the coordination number of the K_A cations is reduced from 12 to 8−10 for all atoms except K(8), which formally retains 12-fold coordination. The BVS values for the K_A atoms do not depart significantly from the nominal value varying in the range of 0.80−1.17 with an average of 0.97.

4. Discussion

The structure analysis of α-K_3AlF_6 confirms the earlier suggestion that the $a = b \approx a_e\sqrt{5}$, $c = 4a_e$ superstructure in the seemingly isostructural room-temperature forms of K_3AlF_6 and $K_3MoO_3F_3$ arises from large amplitude rotations of the $B'X_6$ (B' = Mo, Al; X = O, F) octahedra.[6−8] In α-K_3AlF_6, the AlF_6 octahedra are only slightly deformed, whereas the coordination environment of the K_B atoms is subjected to significant changes. In this sense, the crystal structure of α-K_3AlF_6 is similar to the $Rb_2KB'F_6$ structures, where part of the $B'F_6$ (B' = Cr, Ga) octahedra rotate as rigid units by $\pi/4$ around the c_e axis of the elpasolite cubic subcell, resulting in the $a = b \approx a_e\sqrt{5}$, $c = a_e$ supercell.[8] However, instead of rotation around a single subcell axis, in α-K_3AlF_6, octahedral rotations occur around all three elpasolite subcell axes. The α-K_3AlF_6 structure can be considered to be composed of symmetrically equivalent layers of the AlF_6 octahedra, containing the octahedra rotated by $\pi/4$ around the c_e and a_e or b_e axes. A close comparison revealed that, in both α-K_3AlF_6 and $Rb_2KB'F_6$ structures, the octahedra rotated by $\pi/4$ around the c_e are placed according to the *F*-centered tetragonal $a = b \approx a_e\sqrt{5}$, $c = a_e$ unit cell (Figure 7). The $c = 4a_e$ superstructure in α-K_3AlF_6 arises due to ordered pattern of

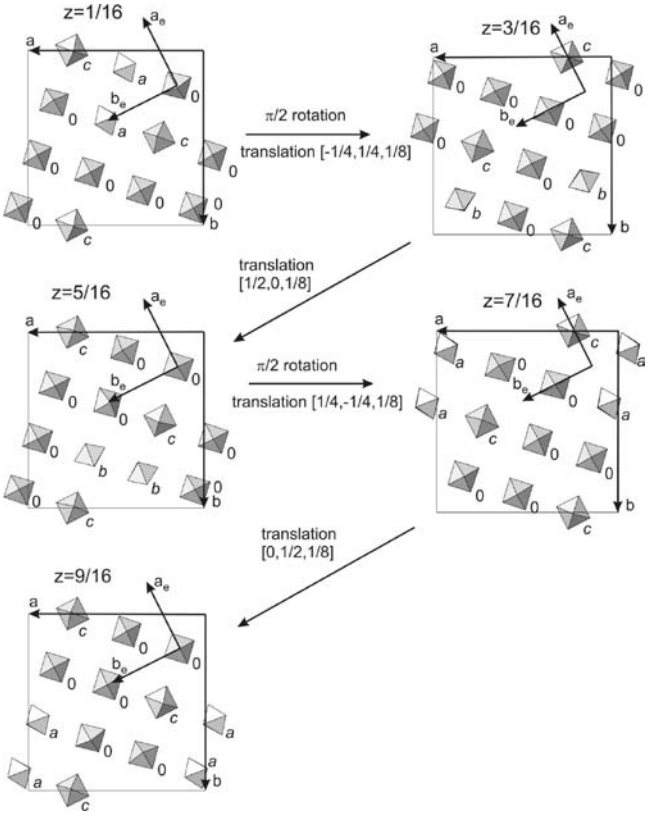

Figure 6. Sequence of the octahedral layers in the α-K_3AlF_6 structure. The 0, *a*, *b*, and *c* notations stand to mark an absence of rotation of the AlF_6 octahedra over $\pi/4$ or rotation around a_e, b_e, or c_e axes, respectively. The tetragonal (**a**, **b**) and cubic elpasolite ($\mathbf{a}_e$, $\mathbf{b}_e$) lattice vectors are shown.

the octahedra rotated around the a_e or b_e axes. The fraction of rotated octahedra in α-K_3AlF_6 is twice as large as that in the $Rb_2KB'F_6$ (B′ = Cr, Ga) structures. As a result, all K_B cations in α-K_3AlF_6 change their octahedral coordination to either a pentagonal bipyramid (CN = 7) or capped pentagonal bipyramid (CN = 7 + 1), whereas in $Rb_2KB'F_6$ (B′ = Cr, Ga), 20% of the K atoms retain their octahedral coordination.

Due to obvious similarity between the ED patterns of α-K_3AlF_6 and $K_3MoO_3F_3$, it would be logical to assume that both compounds have the same ordering pattern of rotated $B'X_6$ octahedra. However, in the case of $K_3MoO_3F_3$, well pronounced structured diffuse intensity was also observed, originating from local ordering of the O and F atoms.[7] Due to the presence of only fluorine anions, such diffuse scattering was never observed for α-K_3AlF_6. A small monoclinic distortion was proposed for both compounds, but the present structural investigation demonstrates that α-K_3AlF_6 most probably retains tetragonal symmetry. However, it is not necessarily true for $K_3MoO_3F_3$, where the monoclinic distortion can be caused by a loss of inversion centers due to off-center displacement of the Mo^{6+} cations in the MoO_3F_3 octahedra, which can be facilitated by trans positions of the F and O atoms in the octahedra.

The crystal structure of α-K_3AlF_6 is beyond the commonly known superstructures arising in B-site ordered $A_2BB'X_6$ (X = F, O) elpasolites and double perovskites that undergo octahedral tilting but maintain the cooperative corner-linked topology. In α-K_3AlF_6, there is no direct link between the rotation directions of the AlF_6 octahedra because the coordination polyhedra around the K_B cations do not behave

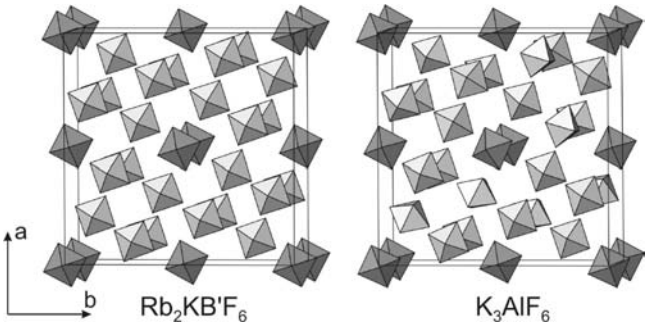

Figure 7. A comparison of the $Rb_2KB'F_6$ (B′ = Cr, Ga) and α-K_3AlF_6 structures. Both structures are drawn in the *F*-centered tetragonal $a = b \approx a_e\sqrt{5}$, $c = a_e$ unit cell. The A and B cations are not shown. The $B'F_6$ and AlF_6 octahedra rotated over $\pi/4$ around the *c* axis are shaded a darker gray.

as rigid units. However, indirect interaction between the rotation modes of the octahedral units can be discussed. Assuming only rotations over a fixed $\pi/4$ angle around one of the a_e, b_e, or c_e axes, several variants can be constructed (Figure 8), representing all possible cases of coordination environments of the B cations with CN = 6, 7, and 8. The B cation can be surrounded by six $B'X_6$ octahedra, keeping their orientations as in the parent elpasolite structure, that is, with four-fold octahedral symmetry axes parallel to the a_e, b_e, or c_e axes (Figure 8a, two $B'X_6$ octahedra above and below the drawing plane are not shown for clarity). The B cation has an octahedral environment with $d(B-X) > d(B'-X)$. Rotation of a single $B'X_6$ octahedron over $\pi/4$ transforms the BX_6 octahedron into the BX_7 distorted pentagonal bipyramid (Figure 8b). Increasing the coordination number up to CN = 8 can occur by the rotation of two $B'X_6$ octahedra in cis positions with respect to the B cation over $\pi/4$ around two perpendicular axes, which can be either noncoplanar (Figure 8c) or coplanar (Figure 8d). In all three cases of CN = 7 and 8, a displacement of the B cations from their ideal positions is possible, resulting in optimization of the interatomic distances between the B cations and X anions, belonging to the $B'X_6$ octahedra not subjected to rotations. The cases shown in Figure 8a−c were experimentally observed in the structures of $Rb_2KB'F_6$ (B′ = Cr, Ga;[9] Figure 8a,b) and α-K_3AlF_6 (Figure 8b,c) elpasolite-type fluorides and $A_{11}B_4O_{24}$ (A = Ca, Sr, B = Re, Os, part of the A positions is vacant) perovskite-type oxides (Figure 8b),[15−17] whereas the rotation of two cis-positioned octahedra around the coplanar axes has not been experimentally found yet. Two more cases should also be considered, which seem to be energetically less favorable (Figure 8e,f). Rotation of two cis-positioned octahedra around the same axis would result in an abnormally short X−X separation and strong electrostatic repulsion. Assuming the elpasolite subcell parameter $a_e \approx$ 8.5 Å and an average Al−F interatomic distance of 1.81 Å, the F−F distance would be as short as 2.38 Å, much shorter than the F−F distance in the AlF_6 octahedra (2.57 Å). Rotation of two octahedra in trans positions (Figure 8d) is

(15) Jeitschko, W.; Moens, H. A.; Rodewald, U. C.; Möller, M. H. *Z. Naturforsch.* **1998**, *53*, 31–36.
(16) Bramnik, K. G.; Miehe, G.; Ehrenberg, H.; Fuess, H.; Abakumov, A. M.; Shpanchenko, R. V.; Pomjakushin, V. Yu.; Balagurov, A. M. *J. Solid State Chem.* **2000**, *149*, 49–55.
(17) Tomaszewska, A.; Müller-Buschbaum, H. *Z. Anorg. Allg. Chem.* **1993**, *619*, 1738–1742.

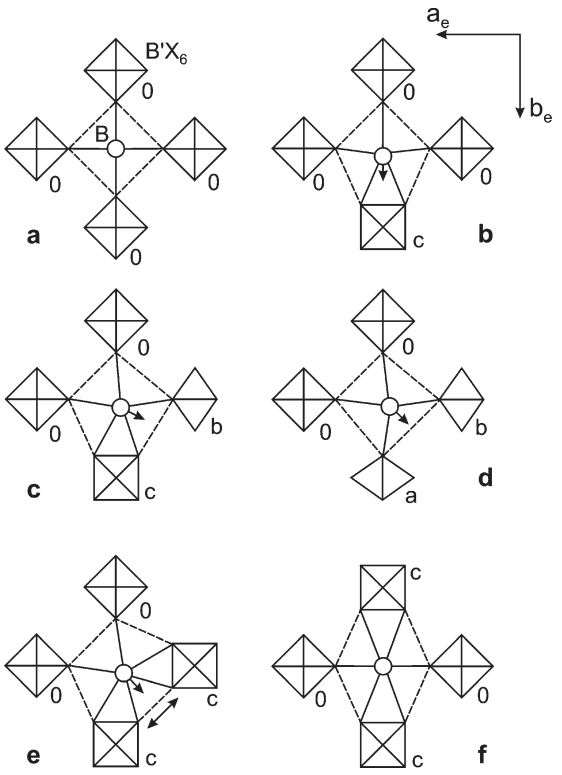

Figure 8. Different modes of the $B'X_6$ octahedra rotations resulting in CN = 6 (a), 7 (b), and 8 (c−f) for the B cations. The octahedra above and below the drawing plane are not shown for clarity. Arrows mark directions of displacements of the B cations. The double-headed arrow indicates short X−X separation.

not compatible with the displacements of the B cations due to the formation of centrosymmetric coordination. Shifting the B cation towards the edge of the rotated octahedron introduces very long distances to the X atoms of a second rotated octahedron at the trans position and does not significantly increase short distances to the X atoms of non-rotated $B'X_6$ octahedra. The same conclusion is applicable to the rotation of octahedra in trans positions around two different axes. Thus, the rotation modes of the octahedral units are mediated by a possibility of relaxation of the B−X bonds due to off-center displacement of the B cations and the anion−anion repulsion between the neighboring $B'X_6$ octahedra. It should be noted that BX_9 polyhedra can be also constructed, for example, by rotation of three *cis*-$B'X_6$ octahedra around different axes, but CN = 9 has not been observed yet in such structures.

The existence of the $A_{11}B_4O_{24}$ (A = Ca, Sr; B = Re, Os) perovskite-type oxides with broken corner-sharing connectivity allows us to assume that other perovskite-like oxides with similar structures would also exist. Although the number of known perovskites and elpasolites with broken corner-sharing connectivity is limited, the analysis of their structures can suggest the key factors defining the stability of such compounds. The tolerance factor $t = (R_A + R_X)/[\sqrt{2}((R_B + R_{B'})/2 + R_X)]$, expressing a mismatch between the A−X and (B,B′)−X interatomic distances, is in the range of t = 0.89−0.93 for such compounds. This tolerance factor falls in the range where octahedral tilting would be expected.

(18) Lufaso, M. W.; Woodward, P. M. *Acta Crystallogr.* **2001**, *B57*, 725–738.

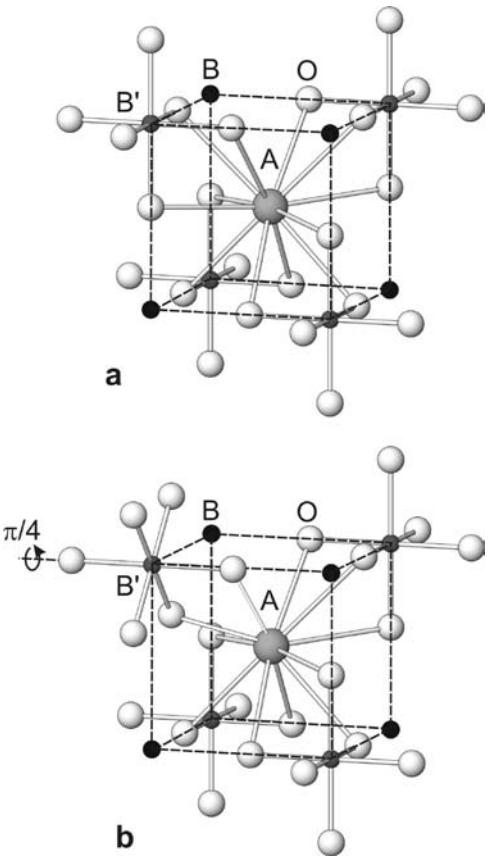

Figure 9. Coordination environment of the A cation in the cubic elpasolite structure (a) and its modification by a rotation of one $B'X_6$ octahedron over $\pi/4$ (b). 1/8 of the cubic elpasolite unit cell is shown.

Prediction of the K_3AlF_6 structure using SPuDS software[18] revealed reasonably low global instability indexes, GII,[19] for at least three tilt systems, $a^-b^+a^-$ (S.G. $P2_1/n$, GII = 0.0103), $a^0b^-b^-$ (S.G. $I2/m$, GII = 0.0016), and $a^-a^-a^-$ (S.G. $R\bar{3}$, GII = 0.0002), although the low GII seen for the latter system does not take into account unfavorably short F−F distances that occur. Thus, the mismatch between the A−X and (B,B′)−X interatomic distances cannot be the main driving force for large octahedral rotations.

We suggest that a difference in ionic radii of the B and B′ cations ΔIR can be used as an indicator of the ability of the B cations to increase their coordination number due to large amplitude rotations of the relatively small $B'X_6$ octahedra. For K_3AlF_6, $K_3MoO_3F_3$, and $Rb_2KB'F_6$ (B′ = Cr, Ga), this difference is remarkably large (ΔIR = 0.76 − 0.85 Å) and becomes only a little smaller for the $A_{11}B_4O_{24}$ (A = Ca, Sr; B = Re, Os) compounds (ΔIR = 0.50−0.66 Å). On going from $K_3MoO_3F_3$ to A_2KMoF_6 (A = K, Rb, Cs, Tl),[20,21] the ΔIR value decreases to 0.71 Å due to the increasing size of the Mo cations upon reduction from Mo^{6+} to Mo^{3+} that stabilizes the undistorted cubic elpasolite structure. The corner sharing of the octahedral framework is restored in double perovskites when the ΔIR value is near or below ~0.5 Å, as it

(19) Salinas-Sanchez, A.; Garcia-Munoz, J. L.; Rodriguez-Carvajal, J.; Saez-Puche, R.; Martinez, J. L. *J. Solid State Chem.* **1992**, *100*, 201–211.

(20) Toth, L. M.; Brunton, G. D.; Smith, G. P. *Inorg. Chem.* **1969**, *8*, 2694–2697.

(21) Hoppe, R.; Lehr, K. *Z. Anorg. Allg. Chem.* **1975**, *416*, 240–250.

occurs in Ca_3ReO_6, Ba_2CaReO_6 ($\Delta IR = 0.48$ Å),[22,23] Ba_2LaRuO_6 ($\Delta IR = 0.50$ Å),[24] Ca_2LaRuO_6 ($\Delta IR = 0.44$ Å),[24] and Ba_2CaOsO_6 ($\Delta IR = 0.45$ Å).[23] Thus, the limiting ΔIR values can be evaluated as $\Delta IR \approx 0.75$ Å for elpasolites and $\Delta IR \approx 0.5$ Å for double perovskites.

The size of the A cation can be considered a secondary factor. A rotation of one of the $B'X_6$ octahedra decreases the coordination number of the A cation by 1 and shortens one of the remaining 11 A−X distances (Figure 9). Reasonably small A cations ($t = 0.89 - 0.93$) would favor such transformation. Increasing t to 0.94−0.98 again stabilizes the cubic elpasolite structure in Cs_2TlMoF_6 and Cs_2KCrF_6 in spite of large ΔIRs of 0.83 and 0.76 Å, respectively.[21,25] However, it should be noted that such structures should be thoroughly re-investigated because the superlattice reflections arising from ordered rotations of the $B'X_6$ octahedra can be easily overlooked due to complex multiple twinning associated with such superstructures. Such twinning was observed for α-K_3AlF_6, $Rb_2KB'F_6$ ($B' = Cr, Ga$), and $K_3MoO_3F_3$.

Acknowledgment. This work was supported by the Russian Foundation of Basic Research (RFBR Grants 07-03-00664-a, 06-03-90168-a). Financial support from the NSF through a Materials World Network grant (MWN-0603128) is gratefully acknowledged. We would like to thank Aziz Daoud-Aladine and Kevin Knight for assistance in collecting the NPD data. A.M.A. is grateful to Ray Withers and Gustaaf Van Tendeloo for fruitful discussion.

Supporting Information Available: A table with positional parameters for the α-K_3AlF_6 structure and a crystallographic information (CIF) file. This material is available free of charge via the Internet at http://pubs.acs.org.

(22) Abakumov, A. M.; Shpanchenko, R. V.; Antipov, E. V.; Lebedev, O. I.; Van Tendeloo, G. *J. Solid State Chem.* **1997**, *131*, 305–309.
(23) Yamamura, Y.; Wakeshima, M.; Hinatsu, Y. *J. Solid State Chem.* **2006**, *179*, 605–612.
(24) Battle, P.D. *Mater. Res. Bull.* **1981**, *16*, 397–405.
(25) Siebert, G.; Hoppe, R. *Z. Anorg. Allg. Chem.* **1972**, *391*, 117–125.